ADVANCES IN ATMOSPHERIC SCIENCES, VOL. 23, NO. 1, 2006, 127–140

Intermediately Complex Models for the Hydrological Interactions in the Atmosphere-Vegetation-Soil System*

ZENG Xiaodong**[1,2,3] (曾晓东), WANG Aihui[1,2,4] (王爱慧), ZENG Qingcun[4] (曾庆存), Robert E. DICKINSON[5], Xubin ZENG[1], and Samuel S. P. SHEN[2]

[1] *The University of Arizona, Tucson, AZ, USA*

[2] *University of Alberta, Edmonton, AB, Canada*

[3] *Institute of Biophysics, Chinese Academy of Sciences, Beijing*

[4] *Institute of Atmospheric Physics, Chinese Academy of Sciences, Beijing*

[5] *Georgia Institute of Technology, Atlanta, GA, USA*

(Received 6 June 2005; revised 22 July 2005)

ABSTRACT

This paper investigates the hydrological interactions in the atmosphere-evegetation-soil system by using the bucket model and several new simplified intermediately complex models. The results of mathematical analysis and numerical simulations show that these models, despite their simplicity, can very clearly reveal the essential features of the rather complex hydrological system of atmosphere-ecosystem-soil. For given atmospheric variables, these models clearly demonstrate multiple timescales, the "red shift" of response spectra, multi-equilibria and limit cycles, bifurcation, abrupt change, self-organization, recovery, "desertification", and chaos. Most of these agree with observations. Especially, the weakening of "shading effect" of living canopy and the wilted biomass might be a major mechanism leading to the desertification in a relatively short period due to overgrazing, and the desertification in a relatively long period or in climate of change might be due to both Charney's mechanism and the shading effect. These ideas could be validated with further numerical simulations. In the paper, some methods for improving the estimation of timescales in the soil water evolution responding to the forcing are also proposed.

Key words: Atmosphere-vegetation-soil system, hydrological process, multi-equilibria, chaos, desertification, shading effect

1. Introduction

The Earth's surface layer (including the biosphere's ecosystems) and the atmospheric boundary layer form a complicated open system. The system receives external energy input by absorbing the solar radiation, and loses energy through its thermal radiation and various kinds of heat exchange with the atmosphere. (Here, the heat exchange with the underlying layers and lithosphere is neglected for simplicity). The system also has momentum and mass exchanges with its surrounding medium. The internal interactions between its internal components such as the atmospheric boundary layer, oceanic boundary layer, land surface layer and the ecosystem are extremely complicated. The variety and complexity of the climate/environment are the consequences of the external energy input and the various external and internal interactions.

Temperature and its thermal regime of the land surface layer are strongly interactive with the atmospheric boundary layer. The source of water (every phase) in the atmosphere is the evaporation from surfaces of the ocean and land, but most of the water in the land surface layer (including the vegetation ecosystems) comes from the atmospheric precipitation. Since the 1950s, the significant influence of soil water and hydrological processes on the climate formation and its evolutionary process has been well explored. For example, this strong influence have been very clearly demonstrated by some early climate simulations carried out by Manabe (1969), Yeh et al. (1984) and

*Invited lecture given at the scientific meeting to celebrate Prof. D-Z Ye's 90th birthday, January 2005, Beijing.

**E-mail: xdzeng@atmo.arizona.edu

many other investigators. Nowadays, the climate system model (CSM) consists of an atmospheric general circulation model (AGCM), oceanic general circulation model (OGCM, including oceanic ice), land surface process model (LSM, including land–cryosphere and ecosystem), and their coupling (by formulations of consistent boundary conditions at the interfaces). The CSM governing equations describe the evolutionary processes of all variables of the climate system such as temperature, water content of different phases, and so on. Since Dickinson's pioneering work on LSMs (Dickinson, 1984), their further development has made rapid progress. Now, we have quite advanced LSMs, such as the two models developed by Dickinson et al. (1993, 1998), Ji's model (1995), and IAP-94 (Dai and Zeng, 1997). Some revisions of these models are reported in Zeng et al. (2001)*, Dai et al. (2003), and Zeng et al. (2002). All these models have comprehensive processes, but their ecosystems and bio-ecological processes are still rather rough and in need of improvement. However, they are all too complicated in the sense that one cannot easily understand the interaction mechanisms in the model without massive computations and elaborative analysis of the huge dataset generated by the numerical simulations. Therefore, it might be difficult to use a complicated LSM to clearly and compactly interpret the features of the land surface system.

This paper reviews some simplified (intermediately complex) models for hydrological interactions in the atmosphere–vegetation–soil system and their results. Such models help to overcome the difficulty of complexity mentioned above. Some of the models and their results have been published (Dickinson et al., 2003; Zeng et al., 2003b, 2004, 2005b; Wang et al., 2003, 2004; and Zeng et al., 2003a). In this paper we will first give a brief review of them and then report some new results. All of our models are based on physical laws, but with parameterization formulations of some micro-mesoscale processes and biophysical processes. The atmospheric variables are prescribed first, and the degrees of complexity of the interactions between the internal components are increased step by step. By so doing, some essential characteristics of the land surface processes, especially the hydrological interactions between the soil and vegetation ecosystems, can be very clearly demonstrated and compactly simplified. We hope that our results with further improvements can be useful for application to the analysis of the complicated and comprehensive LSM models and their numerical simulations, and to the understanding of some basic features of the global environment–ecological systems.

2. Single variable model of soil hydrology

Our analysis starts from the simplest model, viz., the single variable model of soil hydrology (bucket model) developed first by Manabe (1969). This model is still one of the basic models of theoretical interest.

Suppose that there is a horizontally homogeneous soil surface layer (including vegetation, if any). Denote the water content in the whole vertical column with unit horizontal area as W, the atmospheric precipitation as P, evaporation (evapotranspiration, if vegetation exists) as E, and runoff as R, where all P, E and R are per unit time. The uptake of underground water (water table) for the soil surface layer is omitted for simplicity. Thus, we have

$$\frac{dW}{dt} = P - E - R\,. \tag{2.1}$$

This means that the soil surface layer, characterized by its water content W, is an open system with input P and output $E+R$, which is positive and nonlinearly dependent on W and some other properties of the soil and atmospheric boundary layer.

There are two timescales characterizing the evolutionary process of W. One is the input or forcing timescale $t_{\rm f}^*$, determined by the timescale of P; the other is the e-folding timescale (in the literature it is also called the decay timescale or response timescale), t^*, determined by the internal state W and the properties of the soil and atmospheric boundary layer. When P=0, the evolutionary process of W follows t^*.

Since $0 \leqslant W \leqslant W^*$, $0 \leqslant E \leqslant E^*$, where W^* is the so-called field capacity (maximum or saturated water content of the soil) and E^* the potential evaporation (or potential evapotranspiration), we have $E = E^*$ as $W = W^*$ (but E^* also depends on the soil temperature); R is significant only as W is close to W^*; and E is always a leading term in the equation. $t^*= W^*/E^*$ is usually taken in the literature, for example in Serfini and Sud (1987), Delworth and Manabe (1988), and some papers dealing with the statistical analysis of observed climatological data of soil water content (Vinnikov et al., 1996; Entin et al., 2000; Wu et al., 2002). However, as we have mentioned that E and R also nonlinearly depend on W itself, such a determined t^* is only the first approximation of the e-folding timescale and needs to be improved. We will call W^*/E^* as an inherent timescale (because it does not depend on the input P) and give a method for improving the e-folding timescale later.

In reality, the timescale of P ranges from one hour and even shorter (for convective precipitation) to sev-

*Zeng Qingcun, Z. H. Lin and G. Q. Zhou, 2001: Dynamical models and prediction methods for extraseasonal prediction of climatic anomalies (unpublished monograph).

eral days (for continuous precipitation due to a persistent weather system), and the e-folding timescale of soil water ranges from half a month to about two months. This means that $t_{\rm f}^*/t_{\rm f}^* \approx 10^{-1} \sim 10^{-2}$. Therefore the duration of P and the evolutionary process of W can be roughly divided into "fast" and "slow" processes respectively.

In the following we will improve the estimation of the e-folding timescale and investigate the response of W to the input P. Suppose that P is given together with a prescribed atmospheric boundary layer, so that E depends only on W and some properties of the soil layer. One can always take $E = E^* h(y)$, where $h(y)$ is a monotonically increasing function of $y, y \equiv W/W^*, h(0) = 0$, and $h(1) = 1$. Let the basic (or averaged for a relatively long interval of time) variables be $(\overline{W}, \bar{P}, \bar{E}, \bar{R})$ for (W, P, E, R) respectively, the corresponding anomalies be $(\overline{W}w', \bar{P}p', \bar{E}e', \bar{R}r')$ where (w', p', e', r') are nondimensional variables, and the nondimenstional time be denoted by $t' = t/t^*$, where $t^* \equiv W^*/E^*$. From Eq. (2.1) we have the perturbation equation linearized above the basic state as

$$\frac{dw'}{dt'} = -\alpha w' + \beta p' - \gamma r' \,, \tag{2.2}$$

where $\alpha \equiv dh(\bar{y})/dy, \beta \equiv m_{\rm oi}/\bar{y}, \gamma \equiv \bar{R}/(E^*\bar{y}), m_{\rm oi} \equiv \bar{P}/E^*$(the so-called moisture index in climatology), and $\bar{y} \equiv \overline{W}/W^*$. In general we have $O(\alpha) = O(\beta) = O(1)$, and $\gamma = 0 \sim 1$. [Note that the formulation $\bar{E} + \bar{R} = \bar{P}$ is of high accuracy if $\langle y'^2 \rangle$, the long time interval mean of (y'^2), is small compared with $\bar{y}$, which is the case in reality].

From Eq. (2.2) we know that α^{-1} is the nondimensional e-folding time. Hence the improved dimensional e-folding time scale, denoted as t^{**} hereby, is proportional to its first approximation $t^* \equiv W^*/E^*$ as (Wang et al., 2004)

$$t^{**} = \alpha^{-1} t^* \,. \tag{2.3}$$

Because α depends on $\overline{W}$, the improved e-folding timescale t^{**} indeed depends on the input $\bar{P}$ via $\overline{W}$ (the long term mean of the response of water to the input).

$h(y)$ can be well represented by

$$h(y) = (1 - e^{-\varepsilon y})/(1 - e^{-\varepsilon}) \,, \tag{2.4}$$

where ε is an adjustable empirical parameter, and $\varepsilon \geqslant 1$ in general. Therefore $\alpha = dh(\bar{y})/dy$ decreases with $\bar{y}$. In the dry season, $\alpha^{-1} < 1$ and $t^{**} < t^*$ due to the small $\bar{y}$, while in the wet season or in a place with permanent wet soil, we have $\bar{y} \approx 1$, hence $\alpha^{-1} > 1$ and $t^{**} > t^*$. Only in the case of intermediate $\bar{y}$ we have $t^{**} \approx t^*$. This is due to the nonlinearity of dependence of Eon W.

Let r' be neglected for simplicity, and p' and w' represented in spectral form with harmonics $A_p \exp(i\omega t')$ and $A_w \exp(i\omega t')$ respectively, where ω is the nondimensional frequency. Then from Eq. (2.2) we have

$$\eta \equiv \frac{|A_w|^2}{|A_p|^2} = \left(\frac{\beta}{\alpha}\right)^2 \frac{1}{\left[1 + \left(\frac{\omega}{\alpha}\right)^2\right]} \,. \tag{2.5}$$

(see, for example, Delworth and Manabe, 1988; Dickinson et al., 2003; and Wang et al., 2004).

Equation (2.5) shows that $|A_w|/|A_p|$ is negligible for high frequencies ($\omega^2 \gg \alpha^2$), and almost constant for low frequencies ($\omega^2 \ll \alpha^2$). This means that the response spectrum is relatively red ("red noise") compared with the input, which can be considered as a high frequency random noise (or "white noise") if the seasonal variation of precipitation is subtracted. The separate nondimensional frequency is $\omega_s \approx \alpha$. This means that the soil water responds to the precipitation on timescales comparable or longer than t^{**}. In this sense, t^{**} is indeed a good timescale characterizing the response of soil water to the input. The important coupling of soil and atmosphere is in the relatively low frequency domain which is of significance in the climate variability. Note that due to the dependence of α and t^{**} on $\bar{y}$, and since $\bar{y}$ is a slowly varying function of time, t^{**} is also slowly varying.

Since W does not actively respond to the high frequency atmospheric precipitation, the precipitation goes back to the atmosphere by way of evaporation in a relatively longer time interval. The soil layer stores only the portion of low frequency precipitation and influences the atmospheric weather-climate processes via low frequency evapotranspiration.

For weather prediction (up to several days) and short-term climate prediction (for example, prediction of monthly mean variables and up to one or several seasons) using an atmospheric model coupling with an oceanic and land surface model [(Eq. (2.1) is one of the equations of such a model], it might still be difficult to compute the slowly varying components (such as W) with only the statistics (for time intervals comparable with t^*, for example) but not the evolutionary processes of the fast components (such as P), because some terms in the governing equations for the slowly varying components are complicated and not weakly influenced by the atmospheric processes. For example, $h(y)$ in E [or $dh(y)/dy$ in Eq. (2.2)] is also influenced by sunlight, air temperature and humidity and so on in the way of parameterization. And on the timescale of short-term climate prediction, the number of events (for example, the occurrence of P) is not large enough to make stable statistics. Therefore, proper computational methods for integrating the equations of the complicated coupled model are very important.

The study of climate formation and climate change for decadal or longer timescale may require the long term empirical statistics that would show that $P, E,$

and R are highly correlated with E, W, and W with correlation coefficients μ, λ, and ν, and residuals P'', E'', and R'' respectively. This is due to the fact that in such situations the ensemble means of P, E, and R should be almost in balance, and that the left hand side of Eq. (2.1) is negligible. From Eq. (2.1) we have

$$\frac{dW}{dt} + aW = P'' - R'' - (1-\mu)E'' \equiv F\,, \qquad (2.6)$$

where $a \equiv \lambda(1-\mu) + \nu$ is a dimensional constant, depending on geographic region and climatic conditions. F consists of the residuals P'', E'', and R'' and can be considered as a random process with known statistics (Dickinson et al., 2003). Therefore, the evolutionary processes of W as well as its statistics are determined by the parameter a and the statistics of F. The factors that determine a are especially key aspects. With Eq. (2.6) it is possible to compute only the slow processes by introducing some statistics of the fast variables.

The development of dynamically robust statistical climate models and their investigations have also been of considerable interest (see, for example, Hasselmann, 1976; Arnold, 2002).

3. Three-layer interactive model with a prescribed canopy of vegetation

The vertical structure is neglected in model (2.1), hence some complexity is lost, although it is useful in the study of some hydrological aspects in the whole soil column. We now introduce a simple three-layer interactive model [following Dickinson (1984) and modifications by Wang et al. (2003, 2004)]. It consists of the vegetation canopy, the thin surface layer of the soil, and the rooting zone. The controlling variables are the water contents in each layer. The processes included in the model are evapotranspiration (evaporation and transpiration), runoff (or drainage in the canopy layer) and the soil conductive transport of water. The only input is again the known atmospheric precipitation. We have

$$\frac{dW_{\rm c}}{dt} = P_{\rm c} + E_{\rm r} - (E_{\rm c} + R_{\rm c})\,, \qquad (3.1)$$

$$\frac{dW_{\rm s}}{dt} = P_{\rm s} + R_{\rm c} - (E_{\rm s} + R_{\rm s}) - Q_{\rm sr}\,, \qquad (3.2)$$

$$\frac{dW_{\rm r}}{dt} = P_{\rm r} + \upsilon R_{\rm s} - (E_{\rm r} + R_{\rm r}) + Q_{\rm sr}\,, \qquad (3.3)$$

where the subscripts c, s and r denote the quantities of canopy, surface soil layer and rooting zone respectively; $R_i = \delta_i R_{i1} + R_{i2}, R_{i1}$ and R_{i2} are the saturated and subsaturated runoff respectively in the i-layer, $\delta_i = 0$ or 1: $\delta_i = 1$ and R_{i1} occurs as $W = W_i^*$; Otherwise $\delta_i = 0$ and R_{i1}=0, (we have always $R_{c2} = 0$); $0 \leqslant \upsilon \leqslant 1$ is a fraction (to describe the portion of $R_{\rm s}$ that falls from the s-layer down to the r-layer due to gravity); Q_{sr} is the conductive transport from the s-layer to the r-layer; $P_{\rm c} + P_{\rm s} + P_{\rm r} = P, P_{\rm c} = \min(P_{\rm c}^*, P), P_{\rm s} = \min(P_{\rm s}^*, P - P_{\rm c}), P_i^*$ as well as W_i^* and E_i^* are the given saturated values or the permissibly upper bounds of P_i, W_i and E_i respectively, i=c, r, s. Note that $E_{\rm s}$ is the pure evaporation from the soil surface, $E_{\rm r}$ is the water flux sucked by roots of the vegetation and transported to the canopy, and $E_{\rm c}$ is the sum of transpiration and that part of the evaporation of water which is accumulated on the leaves due to the interception of precipitation by the canopy, $P_{\rm c}$. When the precipitation is not too weak, $P > P_{\rm c}^*, P - P_{\rm c}^*$ arrives at the surface soil layer, and a strong precipitation, which is larger than $P_{\rm c}^* + P_{\rm s}^*$, can directly penetrate into the rooting zone due to some large slits in the soil. In reality $P_{\rm r}$ exists, but it has not been considered in all LSMs so far because it is difficult to determine accurately. Note that in this model $P_{\rm c}^*$ is a given constant independent of time, which is why it is called a model with a prescribed canopy. A model with a time varying canopy is given in sections 4 and 5.

The term $Q_{\rm sr}$ is taken as

$$Q_{\rm sr} = \lambda^{-1}\overline{D_{\rm sr}}\left(\frac{W_{\rm s}}{D_{\rm s}^*} - \frac{W_{\rm r}}{D_{\rm r}^*}\right)\,, \qquad (3.4)$$

where $\overline{D}_{\rm sr} = D_{\rm s}^* D_{\rm r}^*/(D_{\rm s}^* + D_{\rm r}^*), D_{\rm s}^*$ and $D_{\rm r}^*$ are the thicknesses of the s-layer and the r-layer respectively, and $W_{\rm r}^*/D_{\rm s}^* = W_{\rm r}^*/D_{\rm r}^*$ in order to guarantee the vanishing of the water exchange when the s and r layers are both saturated. Note that λ is a characteristic timescale for the interaction due to $Q_{\rm sr}$. This means that after time interval $\Delta t = \lambda, (W_{\rm s}/D_{\rm s}^*) - (W_{\rm r}/D_{\rm r}^*)$ is only e^{-1} times its initial volume if there is only the term $Q_{\rm sr}$ on the right hand sides of Eqs. (3.2) and (3.3).

The summation of Eq. (3.1)–(3.3) yields

$$\frac{dW}{dt} = P - E - R\,. \qquad (3.5)$$

This is just the single variable model (2.1), but with $W = W_{\rm c} + W_{\rm s} + W_{\rm r}, E = E_{\rm c} + E_{\rm s}$ (the evapotranspiration of the whole column), and $R \equiv (1-\upsilon)R_{\rm s} + R_{\rm r}$ (the net runoff of the whole column).

We can also take E_i as

$$E_i = E_i^* h_i(y_i)\,, \qquad (3.6)$$

where $h_i(y_i)$ is similar to Eq. (2.4), but the parameter ε for different layers can be different and denoted as $\varepsilon_i; y_i \equiv W_i/W_i^*$, and E_i^* is a given constant depending on the properties of the canopy and soil.

In this three-layer model there are several characteristic timescales: the external forcing (input) (P) timescale $t_{\rm f}^*$ and the three timescales $t_{{\rm f}i}^*$ (due to the partitioning of P into P_i, i=c, s, r); an internal timescale $t_{\rm q}^* = \lambda$, determined by the conductive transport $Q_{\rm sr}$, and the three inherent (or response)

timescales $t_i^*(i$=c, s, r). All these mean that the three-layer model possesses multiple timescales and that the evolutionary processes of the system are more complicated and can be irregular.

It is obvious that $t_{\rm fc}^* = t_{\rm f}^*$, and $t_{\rm fs}^*$ and $t_{\rm fr}^*$ depend on the power spectral distribution of P. The first approximation of t_i^* can be taken as $t_i^* = W_i^*/E_i^*, (i$ =c, s, r), and usually $E_{\rm c}^* \approx E_{\rm s}^* \approx E_{\rm r}^*$ (but $E_{\rm s}^* > E_{\rm c}^* \approx E_{\rm r}^*$) in the arid and semi-arid regions where $W \ll W^*$, and $E_{\rm s}^* < E_{\rm c}^* \approx E_{\rm r}^*$ in the region with very dense canopy, where $W_{\rm s}^* - W_{\rm s}$ and $W_{\rm r}^* - W_{\rm r}$ both are small due to the effect of the strong shading of a dense canopy. In reality, $W_{\rm c}^*$ is two orders of magnitude smaller than $W_{\rm s}^*$ and $W_{\rm r}^*$, and we have $W_{\rm c}^* \ll W_{\rm s}^* < W_{\rm r}^*$, hence $t_{\rm c}^* \ll t_{\rm s}^* < t_{\rm r}^*$. Similar to the analysis in section 2, we know that the high frequency component on the right hand side of Eq. (3.1) is almost in balance, especially $E_{\rm c} - E_{\rm r} \approx P_{\rm c}$, hence $t_{\rm c}^*$ is nearly equal to or even less than $t_{\rm f}^*$. However there is still a low frequency component in $E_{\rm c}$, although relatively small, due to the existence of the term $E_{\rm r}$. It can be proven that in the general case $t_{\rm s}^* < t^* < t_{\rm r}^*$, where t^* is determined by $W^*/E^* \approx (W_{\rm s}^* + W_{\rm r}^*)/(E_{\rm s}^* + E_{\rm c}^*)$, which is nearly equal to that given by Eq. (2.1). In reality, t_q^* is usually about 10–15 days, $t_{\rm s}^*$ 10–30 days, and $t_{\rm r}^*$ 2–6 months, hence the transpiration is more important than the soil surface evaporation in the short-term climate prediction. Note that evolutionary process of $W_{\rm s}$ is also modulated by $Q_{\rm sr}, P_{\rm s}$ and $R_{\rm s}$, and $W_{\rm r}$ by $Q_{\rm sr}, P_{\rm r}$ and $R_{\rm r}$. This means that the response timescales of $W_{\rm s}$ and $W_{\rm r}$ can be different from $t_{\rm s}^* = W_{\rm s}^*/E_{\rm s}^*$ and $t_{\rm r}^* = W_{\rm r}^*/E_{\rm r}^*$ respectively to some large extent and can vary with time (due to the time variations of the $P_{\rm s}$ and $P_{\rm r}$ probabilities). Later, we will give an improved estimation of the response timescales, denoted as t_i^{**} for distinguishing them from their first approximations $t_i^*(i$ =s, r).

Wang et al. (2003) have developed a numerical scheme suitable for solving Eqs. (3.1)–(3.3) and performed numerous numerical simulations with geographical-climatological parameters obtained from high altitude land in the East Asian semi-arid region for the summer season. P is taken as a random distribution and with an almost constant (perpetual) seasonal (stably ensemble) mean. Some results are shown in Figs. 1 and 2. Figure 1 shows very clearly the multiple timescale phenomena and some irregular and complicated structures in the evolution of the system, especially, in $W_{\rm r}$ (and $E_{\rm r}$), large enough disturbances with very low frequencies can be generated (and hence influence the climate variability in the atmosphere by $E_{\rm r}$), even if the external input P is random with a high frequency. Figure 2 shows the power spectral distributions. It can be seen that large amounts of $P, P_{\rm c}, W_{\rm c}$ and $E_{\rm c} - E_{\rm r}$ are located in the domain with periods less than 0.2 months; $W_{\rm r}$ in the domain with periods larger than 3 months; and, despite that the large portion of $E_{\rm r}$ is in the domain with periods larger than 3 months, there still is some non-negligible part of $E_{\rm r}$ in the domain with periods from 0.2 to 3 months; this may be due to the modulations of $P_{\rm r}$ and $Q_{\rm sr}$. The analysis of the simulated time series shows that the e-folding time for the r-layer is close to $t_{\rm r}^*$, but the difference is not sufficiently small. For example, $W_{\rm r}^*/E_{\rm r}^* \approx 160$ days,

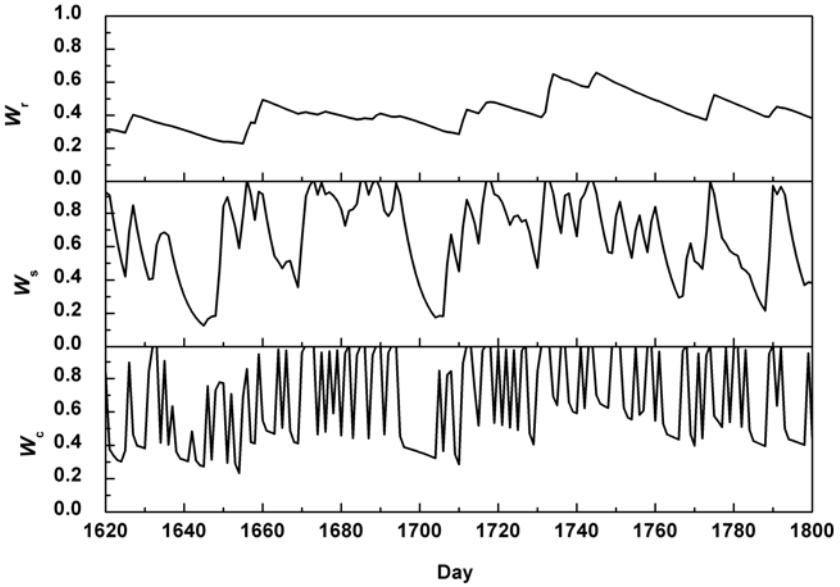

Fig. 1. Daily variations of simulated $W_i/W_i^*(i$=c, s, r). c—canopy, s—surface layer of soil, r—root zone of soil.

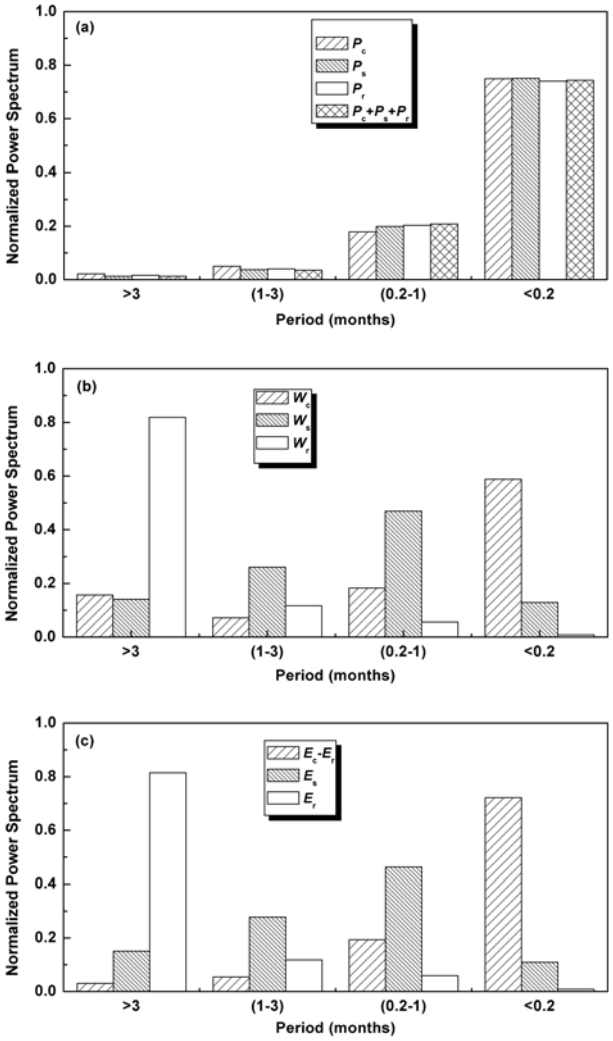

Fig. 2. Normalized power spectral distributions of (a) precipitation and its partitions; (b) water content; and (c) evapotranspiration. The abscissa is the period interval in months.

but the simulated $t_{\rm r}^*$ is very scattered due to the random distribution of $P_{\rm r}$, the ensemble mean of simulated $t_{\rm r}^*$, denoted as $\langle t_{\rm r}^* \rangle$, is only about 90 days, and in 90% of the cases $t_{\rm r}^*$ is within the interval (35, 128) days. This clearly shows that the influence of $Q_{\rm sr}$ and $P_{\rm r}$ on the response timescale is not small, and the first approximation needs to be improved.

Wang et al. (2004) proposed a method to give an improved estimation of the response timescales. They applied again the perturbation method to Eq. (3.1)–(3.3). For the convenience of theoretical analysis and generalization, R_i is approximated by the continuous function as follows

$$R_i = R_i^* g_i(y_i)\,, \tag{3.7}$$

where R_i^* is the upper bound of R_i, and $0 \leqslant g_i \leqslant 1$. Let the climatological state be $(\bar{P}, \bar{P}_i, \overline{W}_i, \bar{R}_i), W_i = W_i^* y_i, y_i' \equiv (W_i - \bar{W}_i)/W^*$ be the perturbation of y_i, etc., so we have the following nondimensional equations, variables and constants:

$$\frac{dy_s'}{d\tau} = \overline{M}_{\rm oi} m_{\rm s} \pi_{\rm s}' - \alpha_{\rm s} y_{\rm s}' + \beta_{\rm s} y_{\rm r}'\,, \tag{3.8}$$

$$\frac{dy_r'}{d\tau} = \overline{M}_{\rm oi} m_{\rm r} \pi_{\rm r}' + \beta_{\rm r} y_{\rm s}' - \alpha_{\rm r} y_{\rm r}'\,, \tag{3.9}$$

$$y_{\rm s}' \equiv W_{\rm s}'/W_{\rm s}^*\,,\ \ y_{\rm r}' \equiv W_{\rm r}'/W_{\rm r}^*\,,$$

$$\pi_{\rm s}' \equiv P_{\rm s}'/\bar{P},\ \ \pi_{\rm r}' \equiv P_{\rm r}'/\bar{P}\,, \tag{3.10}$$

$$\tau \equiv t/t_{\rm rs}^*\,,\ \ t_{\rm rs}^* \equiv t_{\rm s}^* t_{\rm r}^*/(t_{\rm s}^* + t_{\rm r}^*)\,, \tag{3.11}$$

$$\overline{M_{oi}} \equiv \bar{P}/E_{\rm s}^*\,. \tag{3.12}$$

Besides, $m_{\rm s}, m_{\rm r}, \alpha_{\rm s}, \alpha_{\rm r}, \beta_{\rm s}$ and $\beta_{\rm r}$ are all nondimensional parameters [see Wang et al. (2004), for details]. Note that the equation of $y_{\rm c}'$ is omitted here from our consideration because the major function of the c-layer is to reduce the precipitation arriving at the soil surface from P to $P - (P_{\rm c} - R_{\rm c})$, and $P_{\rm c} - R_{\rm c}$ and its perturbation are both small, so this leads to the approximate separability of the evolutionary processes of the s-layer and r-layer from the c-layer. However, the r-layer does directly influence the c-layer via $\overline{E_{\rm r}}$ and $E_{\rm r}'$ (in the low frequency domain).

Letting $\pi_{\rm s}' = \pi_{\rm r}' = 0$, we obtain

$$y_i' = a_i e^{-\alpha_1 \tau} + b_i e^{-\alpha_2 \tau}\,,\ \ (i = {\rm s},\, {\rm r}) \tag{3.13}$$

where $(-\alpha_1)$ and $(-\alpha_2)$ are the two eigenvalues of the matrix

$$M \equiv \begin{bmatrix} -\alpha_{\rm s} & \beta_{\rm r} \\ \beta_{\rm s} & -\alpha_{\rm r} \end{bmatrix}\,,$$

$$\begin{cases} \alpha_1 = \dfrac{1}{2}\{(\alpha_{\rm s} + \alpha_{\rm r}) + [(\alpha_{\rm s} - \alpha_{\rm r}^2) + 4\beta_{\rm s}\beta_{\rm r}]^{1/2}\}\,, \\ \alpha_2 = \dfrac{1}{2}\{(\alpha_{\rm s} + \alpha_{\rm r}) - [(\alpha_{\rm s} - \alpha_{\rm r}^2) + 4\beta_{\rm s}\beta_{\rm r}]^{1/2}\}\,, \end{cases} \tag{3.14}$$

and $\alpha_1 > \alpha_2$. Obviously, (3.13) determines two (dimensional) timescales,

$$t_1^{**} \equiv \alpha_1^{-1} t_{\rm rs}^*,\ \ t_2^{**} \equiv \alpha_2^{-1} t_{\rm rs}^*, \tag{3.15}$$

It can be shown by detailed analysis that $b_{\rm r}$ is much large than $a_{\rm r}$ in (3.13), so that t_2^{**} is an improved estimation of the e-folding timescale for the r-layer.

Taking the same parameters as in the numerical simulations, Wang et al. (2004) obtained $t_{\rm r}^{**} = 123.7$ days, i.e., $t_{\rm r}^{**}$ is located in the interval (35, 128) days, and $t_{\rm r}^{**}$ is closer to $\langle t_{\rm r}^* \rangle$ than $W_{\rm r}^*/E_{\rm r}^*$, although $|t_{\rm r}^{**} - \langle t_{\rm r}^* \rangle|$ is still not small enough. This may be due to the neglecting of the $P_{\rm r}'$ modulation on the timescale in the theoretical analysis.

Now, we investigate the response of soil water to the input of precipitation anomalies. Let

$$\overline{M}_{\rm oi} m_j \pi'_j = A_{\pi j} e^{i\omega\tau} ,$$
$$y'_j = A_j e^{i\omega\tau} = |A_j| e^{i(\omega\tau - \psi_j)} .$$
$$(j = s, r) \qquad (3.16)$$

Substituting (3.16) into (3.8)–(3.9), we obtain

$$A_{\rm s} = \frac{1}{\Delta}[(\alpha_{\rm r} + i\omega)A_{\pi{\rm s}} + \beta_{\rm s} A_{\pi{\rm r}}]$$

and

$$A_{\rm r} = \frac{1}{\Delta}[(\alpha_{\rm s} + i\omega)A_{\pi{\rm r}} + \beta_{\rm r} A_{\pi{\rm s}}] , \qquad (3.17)$$

where

$$\Delta = (\alpha_{\rm s} + i\omega)(\alpha_{\rm r} + i\omega) - \beta_{\rm s}\beta_{\rm r} = |\Delta| e^{i\varphi_\Delta} ,$$
$$|\Delta| = [(\alpha_1^2 + \omega^2)(\alpha_2^2 + \omega^2)]^{1/2} ,$$
$$\varphi_\Delta = \arctan[\omega(\alpha_{\rm s} + \alpha_{\rm r})/(\alpha_{\rm s}\alpha_{\rm r} - \beta_{\rm s}\beta_{\rm r} - \omega^2)] ,$$

and α_1, α_2 are given by Eq. (3.14).

In the simplest case of $A_{\pi{\rm r}} = 0$, we have

$$|A_{\rm s}|^2/|A_{\pi{\rm s}}|^2 = \frac{\alpha_{\rm r}^2 + \omega^2}{(\alpha_1^2 + \omega^2)(\alpha_2^2 + \omega^2)}$$

and

$$|A_{\rm r}|^2/|A_{\pi{\rm s}}|^2 = \frac{\beta_{\rm r}^2}{\alpha_{\rm r}^2 + \omega^2} , \qquad (3.18)$$

$$\psi_{\rm s} = \varphi_\Delta - \varphi_\omega , \ \psi_{\rm r} = \varphi_\Delta , \qquad (3.19)$$

where $\varphi_\omega = \arctan(\omega/\alpha_{\rm r})$. Equation (3.18) is the direct extension of Eq. (2.5). Since $\varphi_\omega > 0$ and $\varphi_\Delta > \varphi_\omega$, we obtain $\psi_{\rm r} > \psi_{\rm s}$, and that means that the phase lag is larger in the deeper layer. This is consistent with the analysis of the observational data (Wu et al., 2004).

In the case of $A_{\pi{\rm r}} \neq 0$, the formulae are slightly complicated. It is better to introduce new variables as follows [see Wang et al., 2004]

$$z'_j = \alpha_{j{\rm s}} y'_{\rm s} + \alpha_{j{\rm r}} y'_{\rm r} \equiv A_{{\rm z}j} e^{i(\omega\tau - \psi_{{\rm z}j})} , \ (j = 1, 2)$$

where $(\alpha_{j{\rm s}}, \alpha_{j{\rm r}})$ is the eigenvector of the matrix M with eigenvalue $(-\alpha_j)$. We have $\psi_{{\rm z}j} = \arctan(\omega/\alpha_j)$, which means that $\psi_{\rm z2} > \psi_{\rm z1}$, i.e., the signal with a larger e-folding time has a larger phase lag [see, Wang et al. (2004), for details]. Because the larger component of z'_2 is $y'_{\rm r}, \psi_{\rm z2} > \psi_{\rm z1}$ leads also to $\psi_{\rm r} > \psi_{\rm s}$.

4. A three-variable ecological-hydrological interactive model

Next, we will investigate the interaction between the vegetation canopy (e.g. leaf area index LAI) and the soil moisture.

Zeng et al. (1994, 1996), presented a maximum simplified grassland ecosystem dynamic model, which consists of only two variables: vegetation biomass M (including living and wilting biomass) and water content inside the grass and the soil W. According to the mass conservation law, the evolutionary equations of both M and W can be derived. Equation (2.1) is just for the evolution of W, but E is also a function of M. Hereafter, his model is referred to as the Ecological-soil Hydrological model (ESH-0). Since ESH-0 is too simple, in order to explain some very important features of the ecosystems, some idealized parameters have to be chosen. In fact, water vapor transpiration together with photosynthesis only occurs in living biomass $M_{\rm c}$, and it sustains the life activity and causes $M_{\rm c}$ to increase. Since the shading of the soil surface by wilting biomass $M_{\rm d}$ reduces the light arriving on the soil surface and thus reduces the surface soil temperature, it also reduces evaporation from the soil surface. Due to the different influences of $M_{\rm c}$ and $M_{\rm d}$ on the soil water and evapotranspiration, the evaporation of the soil surface and the water vapor transpiration of the canopy should be separately considered in the model. Zeng et al. (2003b, 2004, 2005b) developed a grassland ecological dynamic model, which consists of the three variables $M_{\rm c}$, $M_{\rm d}$ and W, and the differences in the influence of $M_{\rm c}$ and $M_{\rm d}$ on W have been taken into account. Hereafter this three-variable ecological-hydrological interactive model is referred to as ESH-1. The model equations are given as follows

$$\frac{dM_{\rm c}}{dt} = \alpha^*(G - D_{\rm c} - C_{\rm c}) , \qquad (4.1)$$
$$\frac{dM_{\rm d}}{dt} = \alpha^*(\beta' D_{\rm c} - D_{\rm d} - C_{\rm d}) , \qquad (4.2)$$
$$\frac{dM}{dt} = P^* p - (E_{\rm s} + E_{\rm r} + R) , \qquad (4.3)$$

where $G, D_{\rm c}$ and $C_{\rm c}$ are the nondimensional growth, wilting, and consuming terms respectively; α^* is the maximum growth rate; $\beta' D_{\rm c}, D_{\rm d}$, and $C_{\rm d}$ are the nondimensional wilting biomass accumulation, decomposition and consuming terms respectively, and $0 < \beta' < 1$ means that only a part of the wilting grass accumulates on the soil surface, (in the model, G and $D_{\rm c}$ are functions of $M_{\rm c}$ and W; $D_{\rm d}$ is a function of $M_{\rm d}$ and W; $C_{\rm c}$ and $C_{\rm d}$ are functions of $M_{\rm c}$ and $M_{\rm d}$ respectively for simplicity); $P^* p$ is the precipitation; $E_{\rm s}$ is the surface evaporation of bare soil and $E_{\rm r}$ is the vegetation transpiration, R is the runoff, and they are functions of W, $M_{\rm c}$ and $M_{\rm d}$. The model assumes that $M_{\rm d}$ is homogeneously distributed on the soil surface, while $M_{\rm c}$ can cover only some parts of the soil surface (the fraction of living grass coverage is denoted as $\sigma_{\rm f}$, and $0 \leqslant \sigma_{\rm f} \leqslant 1$. So $E_{\rm s}, E_{\rm r}$ and R can be expressed by a product of two functions, one of them only depends on $M_{\rm d}$ and the other depends on $M_{\rm c}$ and W.

All terms on the right hand side of Eqs. (4.1)–(4.3) can be derived and expressed by parameterization formulas, based on the consideration of macroscopic and

microscopic physical and biophysical aspects of photosynthesis, wilting process and evapotranspiration and some mathematical-logical constraints. For example, when the atmospheric climate conditions and Planetary Boundary Layer (PBL) are known, the net photosynthesis productivity is $\alpha' R_{\rm pa} G_1(x) G_2(y)$, where $R_{\rm pa}$ is photosynthetic active radiation, $0 \leqslant G_1 \leqslant 1, 0 \leqslant G_2 \leqslant 1, x \equiv M_{\rm c}/M_{\rm c}^*, y \equiv W/W^*$, and $M_{\rm c}^*$ and W^* are the maximum value of the living biomass and the maximum water content respectively; G_1 and G_2 are monotonically increasing functions of x and y respectively; $G_1(0) = G_2(0) = 0, G_1(\infty) = G_2(\infty) = 1$ and $\alpha^* = \alpha' R_{\rm pa}$. Similarly, $D_{\rm c}$ is proportional to $D_1(x)D_2(y), D_1(0) = 0, D_1(\infty) \to \infty, D_2(0) \to \infty, D_2(\infty)$ is finite; $D_{\rm d}$ is a function of $z, z \equiv M_{\rm d}/M_{\rm d}^*$, where $M_{\rm d}^*$ is the maximum accumulation of wilted biomass. Considering the natural processes and human activity, it is reasonable to assume that $C_{\rm c}(0) = C_{\rm d}(0) = 0$ and $C_{\rm c}(\infty)$ and $C_{\rm d}(\infty)$ are bounded. The above analyses almost give the basic form of the functions, which can be approximated by some well-known functions and dimensionless parameters. According to the numerical sensitivity experiments carried out by Zeng et al. (2005b) the solution is insensitive to the specific form of these functions, but sensitive to the model nondimensional parameters representing different soil-vegetation properties. Furthermore, it can also be given as

$$E_{\rm s} + E_{\rm r} = E_{\rm s}^* [e_z(z) e_{\rm s}(x, y) + \varphi_{\rm rs} e_{\rm r}(x, y)] , \qquad (4.4)$$

where $e_{\rm z}(0) = 1, e_{\rm z}(\infty) = 0, e_{\rm s}(x, 0) = 0, e_{\rm s}(0, \infty) = 1, e_{\rm s}(\infty, \infty)$ is finite but equal to or less than 1, $e_{\rm r}(x, 0) = 0, e_{\rm r}(0, y) = 0$, and $e_{\rm r}(\infty, \infty) = 1$. So the general features of $E_{\rm r}$ and $E_{\rm s}$ can be defined. $E_{\rm s}^*$ is the potential evaporation of bare soil, and $E_{\rm r}^* \equiv \varphi_{\rm rs} E_{\rm s}^*$ is the potential transpiration of vegetation without wilted biomass. Both $E_{\rm s}$ and $E_{\rm r}$ approach $E_{\rm s}^*$ and $E_{\rm r}^*$ respectively as $x \to \infty$ and $y \to \infty$. Note that $\varphi_{\rm rs}$ and $1 - e_{\rm s}(\infty, \infty) \equiv \kappa_1$ are two important parameters which represent the shading effect of living biomass. Wilted biomass mainly reduces the solar radiation arriving at the land surface. Similarly to the transmittance, $e_{\rm z}(z)$ can be expressed as

$$e_{\rm z}(z) = e^{-\varepsilon_z z} , \qquad (4.5)$$

where the parameter ε_z characterizes the shading effect of wilted biomass (resulting in the decrease of soil surface temperature). Here, we do not list all of the formulas in detail, so interested readers can refer to Zeng et al. (2003b, 2004; 2005 a, b).

Due to the nonlinear interaction between the vegetation and soil hydrology, ESH-1 is actually a complicated system, and some typical properties inherent in a nonlinear complicated system can be manifested, such as self-organized processes, desertification, multi-equilibrium or limit cycles, bifurcation, abrupt changes and chaos.

Without consideration of annual variation, i.e., when only the annual mean or summer average (climatological ensemble seasonal mean in the Northern Hemisphere monsoon region) is concerned, for a given soil and vegetation type and properties, all the nondimensional parameters are known as constants, which can be derived by theoretical methods or calculated from observational data via the inverse methods. In this case, Eqs. (4.1)–(4.3) have equilibrium solutions, and they vary with precipitation P^* (independent of time) or its equivalent moisture index (nodimensional parameter) $M_{oi} = P^*/E_{\rm s}^*$. As an example, the result for a typical grassland of Inner Mongolia is shown in Fig. 3 (where M_{oi} refers to μ) (Zeng et al., 2005a). The figure also shows the observed living biomass (expressed by vertical segments). The observed μ and vegetation type are also shown in Fig. 4 (modified with permission from Chinese Academy of Sciences, 1985). It can be seen from these two figures that the theoretical result and the observations are well in agreement. In particular, (1) the existence of grassland requires that the moisture index be higher than a critical value μ_1 (abut 0.3, e.g., annual precipitation is about 300 mm), and as $\mu < \mu_1$ there is an idealized desert (in nature some other species tolerant of the arid environment and small shrubs exist, so $x \neq 0$, but they are not included in the model); (2) in the range of $\mu > \mu_2$, there is good grassland and the living biomass increases with μ; (3) for $\mu_1 < \mu < \mu_2$, there are two stable equilibrium states: one is desert, the other is grassland. In these regions, the actual biological state depends on the long term evolution and land use, and in particular, the overuse of existing grassland might eventually lead to desertification. All of these are in agreement with the actual situation in Inner Mongolia, where in the range of $\mu_1 < \mu < \mu_2$, indeed some places are definitely grasslands, but others are desert (sandy land) due to overgrazing [e.g., Hunshandake Desert (sandy land) and Keerqin Desert (sandy land) etc.]

In addition, a method to determine $\varphi_{\rm rs}$ via inverse methods from incomplete and unconventional meteorological data has also been given by Zeng et al. (2005a). In Inner Mongolia, $\varphi_{\rm rs}$ lies between 0.5 and 0.7. This is consistent with the very few but very valuable data from direct observations (e.g., Song, 1997). From this point, it can be considered that the model is of practical use. The results also show that the wilted biomass can reduce evapotranspiration, thus sustain soil wetness. This is also in agreement with the practices in Northern China.

In the study of the interannual and interdecadal climate-ecological changes, all the parameters can also be approximately regarded as time invariant for a given geographical region, but M_{oi} (or μ) may possess a long time term trend with some random variations

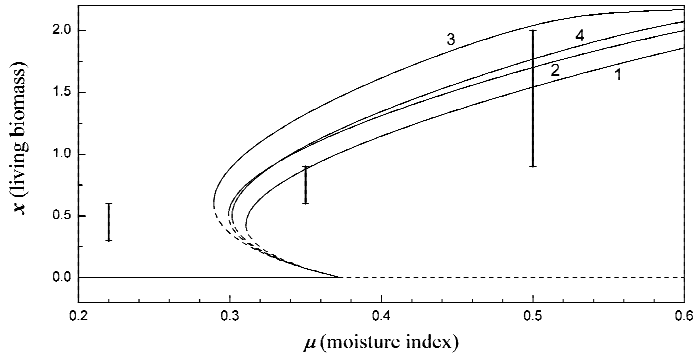

Fig. 3. The dependence of the equilibrium living biomass x on the moisture index μ. The solid and dashed lines refer to the stable and unstable equilibrium states respectively. The vertical segments show the observed living biomass, but the grass in μ <0.3 belongs to another species. Curves 1–4 correspond to the cases of (κ_1, φ_{rs})=(0.3, 0.7), (0.4, 0.6), (0.5, 0.5), and (0.7, 0.7). (Modified with permission from Zeng et al., 2005a)

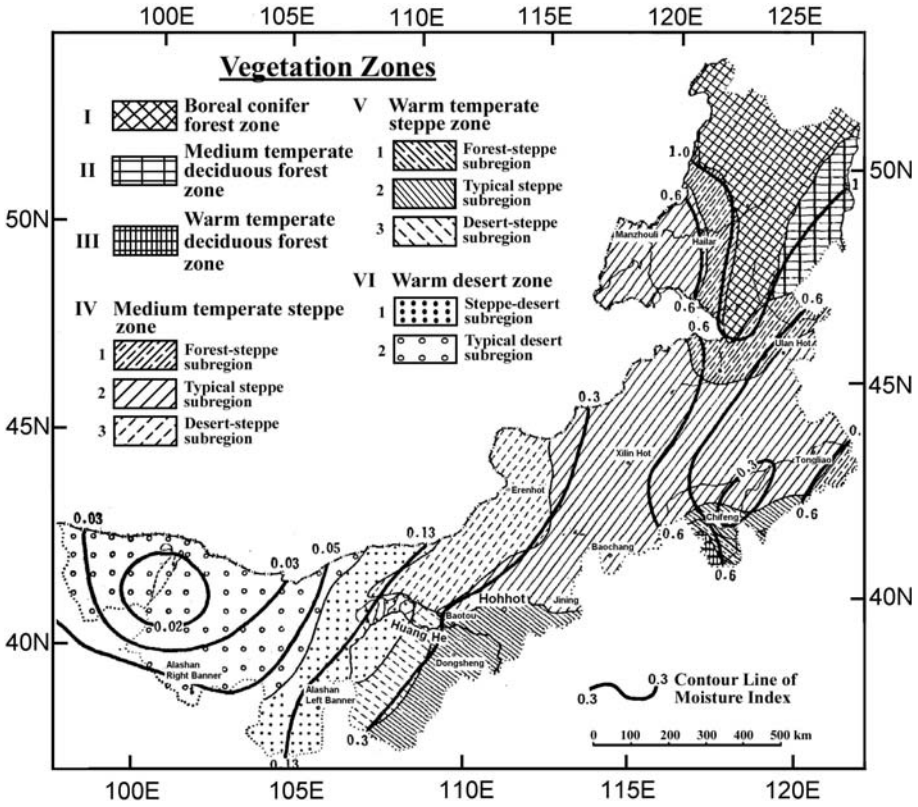

Fig. 4. Distribution of vegetation zone and moisture index in Inner Mongolia. (modified with permission from Chinese Academy of Sciences, 1985).

superimposed upon it. Zeng et al.* carried out some numerical simulations, and the results are shown in Fig. 5. It can be seen that in the region with the moisture index close to the critical value, the grassland ev-

*Zeng X. D., X. B. Zeng, S. S. P. Shen, and R. E. Dickinson, 2004: Multiple equilibrium states and the abrupt transitions in a dynamical system of soil water interacting with vegetation. presented at the CCSM/BGC Group Meeting, 30 March, 2004, Boulder. (unpublished).

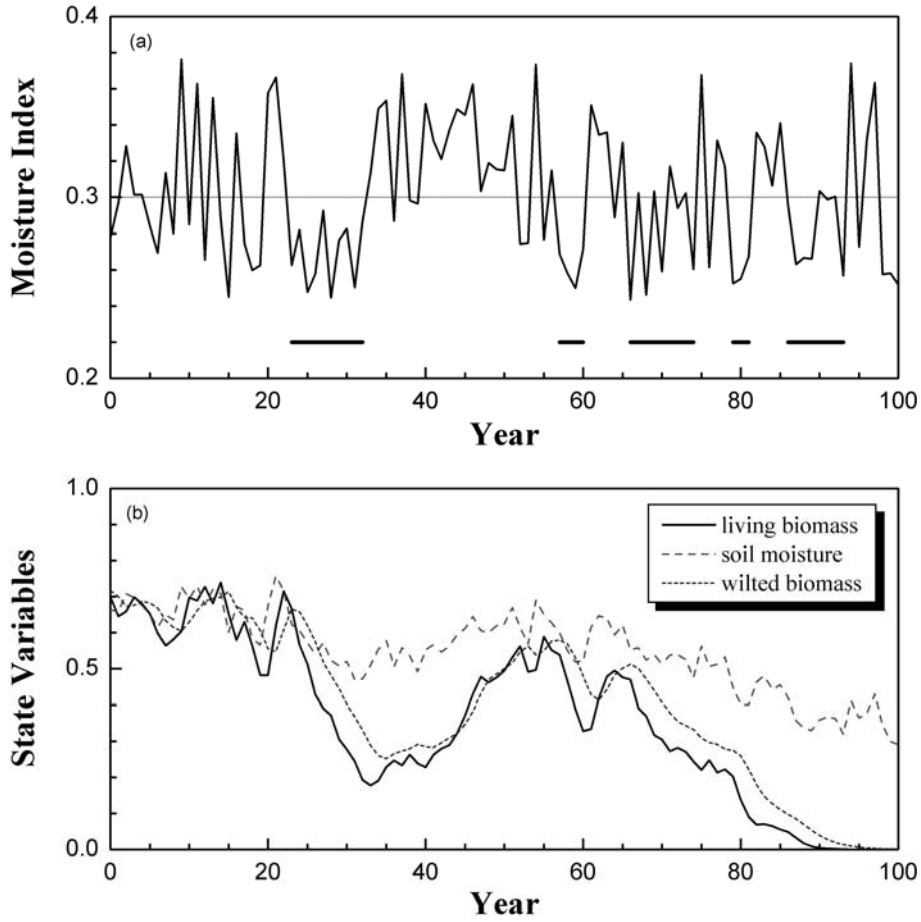

Fig. 5. The desertification of existing grassland under a random fluctuating moisture index. (a) The 100-year trail of annual moisture index μ. The long-term average of μ is μ_{ave}=0.31, and the perturbation $|\Delta\mu(t)| < 0.07$. The horizontal bars indicate the drought periods within which most of the moisture indexes are under the critical value μ_1=0.3. (b) The trails of the annual averages of state variables. The initial state of (x, y, z) is set to the stable equilibrium state of grassland at μ=0.31. The ecosystem finally becomes a desert around year 93.

entually becomes a desert due to insufficient living biomass after many occurrences of severe droughts.

5. Five-variable ecological-hydrological interactive model

Since evaporation and transpiration occur in different layers of the soil-vegetation system with different mechanisms, it is better to improve ESH-1 by dividing the system into three layers: vegetation, soil surface and root zone of soil. The first layer contains three variables: $M_{\text{c}}, M_{\text{d}}$, and W_{c}; the latter two layers are described by W_{s} and W_{r}. Thus a five-variable model, referred to as ESH-2, has been developed (Zeng et al., 2003a) based on Eqs. (4.1), (4.2) and (3.1)–(3.3), where P_{c} (or P_{c}^*) and R_{c} (or R_{c}^*) depend on M_{c}; E_{c} (or E_{c}^*) depends on M_{c}, W_{c} and W_{r}; E_{s} (or E_{s}^*) depends on M_{c}, M_{d} and W_{s}; E_{r} (or E_{r}^*) depends on M_{c} and W_{r} (and also depends on M_{d} due to the influence of soil temperature); and R_{s} (or R_{s}^*) depends on $W_{\text{s}}, M_{\text{c}}$, and M_{d}.

In order to filter the very small high frequency noise in M_{c} and M_{d}, the five-layer model can be simplified by assuming that all terms on the right hand side of Eqs. (4.1) and (4.2) depend only on M_{c}, M_{d} and W_{r} (but W_{c} and W_{s} are not explicitly included there) and that the right hand side of Eq. (3.1) is in balance. Therefore Eqs. (3.1)–(3.3) are modified as

$$P_{\text{c}} - (E_{\text{c}} - E_{\text{r}}) - R_{\text{c}} = 0\,, \tag{5.1}$$

$$\frac{dW_{\text{s}}}{dt} = P_{\text{s}} + R_{\text{c}} - E_{\text{s}} - Q_{\text{sr}} - R_{\text{s}}\,, \tag{5.2}$$

$$\frac{dW_{\text{r}}}{dt} = P_{\text{r}} + \nu R_{\text{s}} - E_{\text{r}} + Q_{\text{sr}} - R_{\text{r}}\,, \tag{5.3}$$

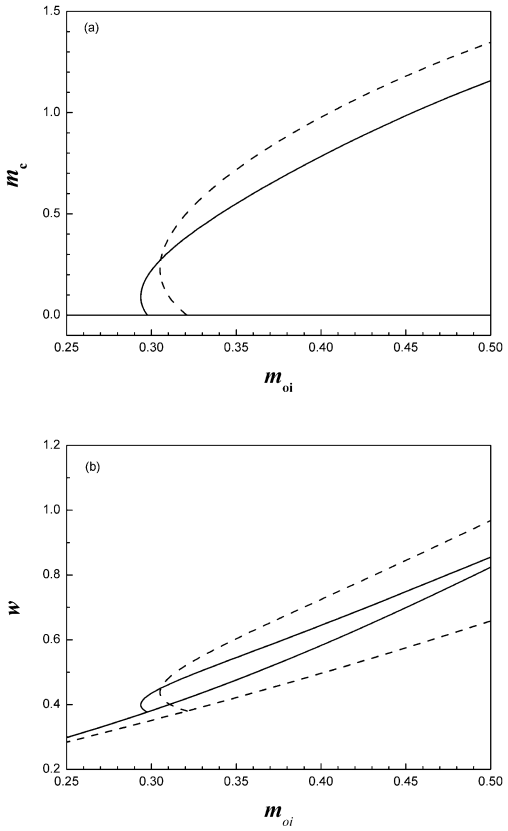

Fig. 6. Bifurcation diagrams: comparison of the equilibrium states between model EH-2 (solid lines) and model EH-1 (dashed lines).

As we have discussed in section 3, from the theoretical point of view, the effect of Eq. (3.1) on W_s and W_r is equivalent to reducing the precipitation reaching the soil surface from P to $P-(P_c-R_c)$. Hence, we can approximately take $P_c = (P_c^*/P^*)\pi_c'$ and $R_c = 0$, where P_c^* is a monotonic increasing function of the leaf area index (LAI) or M_c, and π_c' a dimensionless variable. Eqs. (4.1), (4.2), (5.2) and (5.3) form a differential dynamic system. As $P(t)$ and the initial conditions are given, $M_c(t), M_d(t), W_s(t)$, and $W_r(t)$ can be calculated by numerical methods, and the substitution of them into (5.1) yields $E_c(t) = P_c(t) + E_r(t) - R_c(t)$.

Since ESH-1 can capture the essential features of the vegetation-soil hydrological interactive system, it is easy to imagine that these features can also be simulated by ESH-2, but some quantitative differences may exist.

When $P_i (i = \text{s, r})$ are both constant, M_c, M_d, W_s and W_r all approach their limit values (equilibrium states), and bifurcations exist also in ESH-2. For comparison, Fig. 6 shows the equilibrium states and bifurcation diagrams in ESH-1 and ESH-2, where $m_c \equiv x, w \equiv (W_s+W_r)/(W_s^*+W_r^*)$, and the moisture index is denoted as m_{oi}.

When P and parameters such as α^*, etc., are all periodic functions of t with the same period, the solutions of ESH-2 approach limit cycles (periodic functions of t with the same period). As $M_{oi} > (M_{oi})_2, M_c \neq 0$ (grassland with annual variation); as $M_{oi} < (M_{oi})_1 < (M_{oi})_2, M_c$ finally tends to 0 (the desert state) in spite of some annual variations with $M_c \neq 0$ in several beginning cycles. (The figures are not presented here.)

The result is somehow complicated when P consists of random variations representing the interannual and interdecadal variabilities. Figure 7 shows a typical chaotic phenomenon and recovery of the ecosystem by self-organization, where M_{oi} is only fluctuating around $(M_{oi})_1$ and $(M_{oi})_2$ without a long-term tendency of increasing or deceasing $\bar{P}$. (Note that in the figure all variables and parameters are nondimensional, $m_c \equiv M_c/M_c^*, w \equiv W/W^*, W = W_s + W_r, W^* = W_s^* + W_r^*$, and M_{oi} is denoted as m_{oi}). Both m_c and w vary with time in responses to the variation of m_{oi}. In particular, both m_c and w are larger than the corresponding values of the equilibrium state during the wet years $(m_{oi} > (M_{oi})_2)$, and smaller than the equilibrium values during the drought years $(m_{oi} < (M_{oi})_1)$. It is very interesting to point out that it is still possible for the grassland to recover and exceed the equilibrium value within the coming wet years, although m_c decreases and becomes very small after the stress of several severe drought years.

6. Some discussions on the further improvement of the models and the study of complexity

Models ESH-1 and ESH-2 have only a simple single vegetation ecosystem, which consists of only one species or a community of species with almost the same characteristics. So there exist only two stable ecosystem regimes: vegetation and ideal desert. However, in reality, many different species co-exist and compete among themselves. It is not difficult to take these into account in Eqs. (4.1) and (4.2), but different species have different G, D_c, C_c, D_d, C_d, and different α^* and β^*. Besides, in order to form a closed set of equations, some constraints have to be imposed: the species share definitely limited resources such as space, sunlight, water and nutrients. The interactions between different species, besides competition, can also be considered in the terms G, etc. These lead to the domination of one (or some) species with the disappearance of other species for a given climate-environment condition and a variety of ecosystems with different climate-environment conditions. The new version of CLM and other current biospheric models have included the mechanism of competition, which is rather simple in the present and needs to be improved in the future.

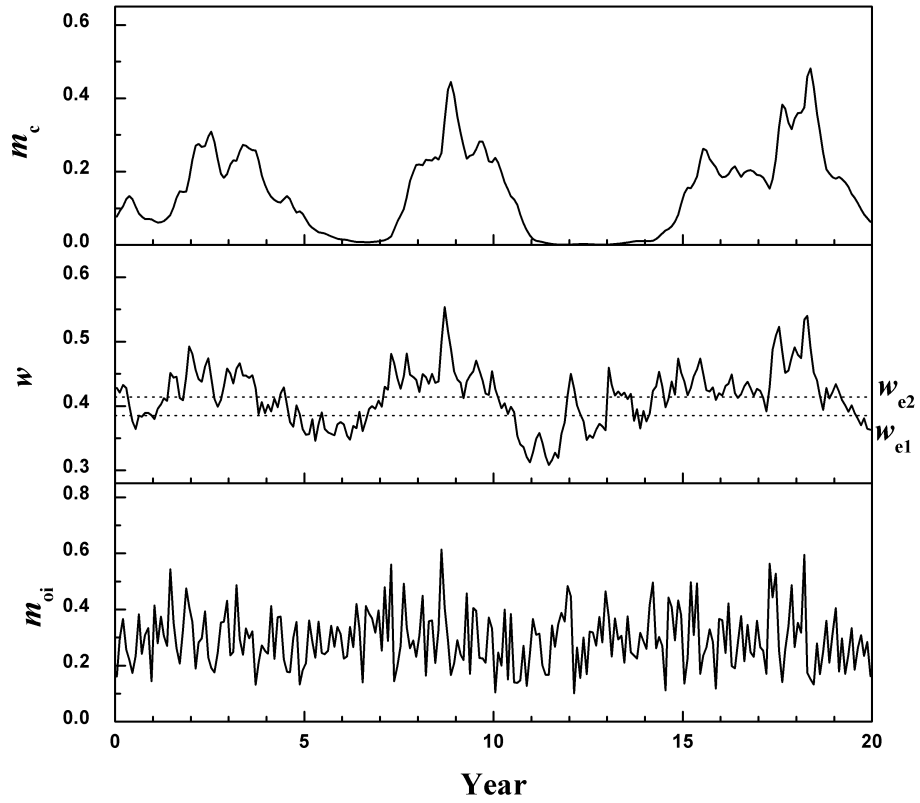

Fig. 7. The temporal variations of $m_c(t), w(t)$ and $w_r(t)$ under a given random precipitation input (equivalently, moisture index $m_{oi}(t)$, and $\overline{m}_{oi} = 0.295$ which is very close to the bifurcation region. w_{e1} and w_{e2} are the values of soil water for the unstable and stable equilibrium state of grassland. The living biomass changes dramatically, can drop to near 0 if w is less than w_{e1} for a long period, and can recover when w is large enough.

The formulation of runoff should also be improved, especially over regions with varying topography. In these cases, there usually is runoff, viz., the water flow in the soil layer. When the soil water is saturated, the abundant water flows down along the slope due to the action of gravity, and in general, the water flux can be represented as $q = -K\nabla z_s$, where z_s is the elevation above sea level and K is the hydraulic conductivity. For a small catchment, this formula is very simple but very practical. However, for a large area, which is represented as a grid point in LSM, the inhomogeneous topography and soil properties lead to the necessity of considering the statistics of these variables and some difficulties in determining z_s and K. A new scheme for improving the runoff term in CLM has recently been proposed by Dickinson*. Moreover, for a comprehensive description, the influence of a variable water table should also be taken into account in some regions. Besides, in the extratropical latitudes, the soil water is not always in a saturated state, but there is subsaturated runoff (water flow in the soil), although small. Hence, the coefficient K depends also on the gradient of water content, ∇w, and a better formula might be given as

$$K = K_0 \left(1 - b\frac{\nabla w \cdot \nabla z_s}{|\nabla w \cdot \nabla z_s|}\right) , \tag{6.1}$$

where $w \equiv W/W^*$, and K_0 and b are two local empirical coefficients. Now, we have

$$-R = R_1 + R_2 , \tag{6.2}$$

which $R_1 = -\nabla \cdot (K\nabla z_s)$, which is further simplified by Dickinson as

$$R_1 = K_0 D|\nabla z_s|/a , \tag{6.3}$$

where a is the ratio of the area facing the slope, and D is another coefficient and might depend on $\nabla w \cdot \nabla z_s$ if Eq. (6.1) is taken. This amount of water, R_1, should be injected into the next grid along the downward direction of the slope. As for R_2, resulting from the gradient of w, we suggest the following formula

$$R_2 = \nabla \cdot (K_2 \nabla w) , \tag{6.4}$$

*Dickinson R. E., 2004: Improving runoff in CLM, unpublished

where K_2 is another conductivity coefficient. R_2 exists, even if there is no slope, and acts also as a smoothing operator.

It should be pointed out that $(-R)$ is not always a sink of soil water but a source in some areas where the water flow in the soil layer exists.

Some improvement in computing evaporation and evapotranspiration in CLM might be useful too, because the roots' capacity to take up soil water for the leaves, hence evapotranspiration, varies with their age and the season, and the mass of the roots as well as the water flux from the roots to the leaves are not necessarily proportional to the mass of the canopy. Besides, when the interactions between the atmosphere and the soil-vegetation layer are investigated, one must add one equation for soil temperature and some equations for the physical processes in the atmospheric boundary layer as well as the continuity of fluxes. These are included in CLM but not in our simplified models yet.

By using a fully-coupled whole atmosphere and land surface model, one is able to study the mutual interactions of the climate and environment-ecosystems and their bilateral influences, especially the changes due to human activities. Charney (1975) proposed a mechanism of desertification resulting from the overuse of grassland. This theory suggests that the overuse of grassland increases the albedo, and as a consequence, the atmospheric precipitation is reduced, eventually leading to desertification. This may be referred to as the "mechanism of the albedo effect". This mechanism is generally accepted by the investigators, and seems to be well verified by many simulations using currently developed coupled models. However, in all these models, no wilted biomass or its "shading effect" are included. Our models, ESH-1, ESH-2 and their associated theoretical studies (Zeng et al., 2003, 2004, a, b), clearly show that the decrease of the shading effect can result in rapid desertification. This may be referred to as the "mechanism of the shading effect". This mechanism is especially significant as the cover of wilted biomass is taken into account. Note that in the arid and semiarid zones and their surrounding areas, the wilted biomass cannot be quickly decomposed and mixed with the soil. Its influence on the evapotranspiration is very different from that of the living biomass and soil surface, and its shading effect is likely very important in those areas.

Both mechanisms probably exist in the process of desertification. Considering that the desertification mostly occurs in the arid and semiarid zones, we suppose that the desertification resulting from human activities is first due to the mechanism of the shading effect, and that the mechanism of the albedo effect becomes significant and important only over a long period or due to climate change. It may be very interesting to perform some numerical simulations with regard to this issue.

Acknowledgments. This work was supported by the China National Science foundation (Grant No. 40233027); NOAA Office of Global Programs, NASA (NAGA-13322) and the U. S. National Science foundation (ATM 0301188); and the Chinese Academy of Sciences' Overseas Assessor's Grant and Well-Known Overseas Chinese Scholar Grant. Aihui Wang was supported by a WMO fellowship. The authors are very grateful for the assistance of Gang Zhao of the Inner Mongolia University, and Dongling Zhang, Dewang Fu, and Xiaoyun Xu of the Institute of Atmospheric Physics, Chinese Academv of Sciences, in the preparation of this manuscript and for the two reviewers' comments and suggestions in improving the revised paper.

REFERENCES

Arnold, L , 2002: Linear and nonlinear diffusion approximation of the slow motion in systems with two time scales. IUTAM Symposium on Nonlinear Stochastic Dynamics, University of Illinois at Urbana-Champaign, N. Sri Namachchivaya, Ed., Kluwer, Dordrecht, 5–18.

Charney, J. G., 1975: Dynamics of deserts and drought in Sahel. *Quart. J. Roy. Meteor. Soc.*, **101**, 193–202.

Chinese Academy of Sciences Comprehensive Survey Group of Inner Mongolia and Ningxia Autonomous Regions, 1985: *The Inner Mongolia Vegetation.* Science Press, Beijing. (in Chinese)

Dai Yongjou, and Zeng Qingcun, 1997: A land surface model (IAP94) for climate studies, Part I: Formulation and valiadation, off-line experiments. *Adv. Atmos. Sci.*, **14**, 433–460.

Dai, Y. J., and Coauthors, 2003: The Common Land Model (CLM). *Bull. Amer. Meteor. Soc.*, **84**, 1013–1023.

Delworth, T., and S. Manabe, 1988: The influence of potential evaporation on the variabilities of simulated soil wetness and climate. *J. Climate*, **1**, 523–547.

Dickinson, R. E., 1984: Modelling evapotranspiration for three-dimensional global climate models. *Geophysical Monograph*, **29**, 58–72.

Dickinson, R. E., A. Henderson-Sellers, and P. J. Kennedy, 1993: Biosphere-Atmosphere Transfer Scheme Version 1e as Coupled to the NCAR Community Climate Model. NCAR Tech. Note 387+STR, 77pp.

Dickinson, R. E., M. Shaikh, R. Bryant, and L. Graumlich, 1998: Interactive canopies for a climate model. *J. Climate*, **11**, 2823–2836.

Dickinson, R. E., Guiling Wang, Xubin Zeng, and Zeng Qingcun, 2003: How does the partitioning of evapotranspiration and runoff between different processes affect the variability and predictability of soil moisture and precipitation? *Adv. Atmos. Sci.*, **20**, 475–478.

Entin, J., A. Robock, K. Y. Vinikov, S. E. Hollinger, S. Liu, and A. Namkai, 2000: Temporal and spatial scales of observed soil moisture variations in the extratropics. *J. Geophys. Res.*, **105**, 11864–11877.

Hasselmann, K., 1976: Stochastic climate models, part I: Theory. *Tellus*, **28**, 473–485.

Ji, J. J., 1995: A climate-vegetation interaction model: Simulating physical and biological process at the surface. *Journal of Biogeography*, **22**, 2063–2068.

Manabe, S., 1969: Climate and the ocean circulation, I: The atmospheric circulation and the hydrology of the earth's surface. *Mon. Wea. Rev.*, **97**, 739–774.

Serafini, Y. V., and Y. C. Sud, 1987: The time scale of the soil hydrology using a simple water budget model. *J. Climate*, **7**, 581–591.

Song Bingyu, 1997: A study on evaporation and transpiration of grassland plant community. *Climatic and Environmental Research*, 1997, **2**, 222–235. (in Chinese)

Wang, A. H., X. D. Zeng, X. B. Zeng, S. S. P. Shen, and Q-C. Zeng, 2003: Dynamics and numerical simulations of hydrological vegetation-soil interaction. *Proceedings of ICCP6-CCP2003*, Rinton Press Inc., Beijing.

Wang, A. H., X. B. Zeng, S. S. P. Shen, Q-C. Zeng and R. E. Dickinson, 2004: Time scales of land surface hydrology, to appear in *Journal of Hydrometeorology*, 2005.

Wu, W., M. Geller, and R. E. Dickinson, 2002: The response of soil moisture to long-term variability of precipitation. *J. Hydrometeor.*, **3**, 604–613.

Yeh, T.-C., R. T. Wetherald, and S. Manabe, 1984: The effect of soil moisture on the short-term climate and hydrology change—A numerical experiment. *Mon. Wea. Rev.*, **112**, 474–490.

Zeng Qingcun, Lu Peisheng, and Zeng Xiaodong, 1994: Maximum simplified dynamic model of grass field ecosystem with two variables. *Science in China*(B), **37**, 94–103 .

Zeng Q.-C., and X. D. Zeng, 1996: An analytical dynamic model of grass field ecosystem with two variables. *Ecological Modelling*, **85**, 187–196.

Zeng, X-B., M. Shaikh, Y-J. Dai, and R. E. Dickinson, 2002: Coupling of the Common Land Model to the NCAR Community Climate Model. *J. Climate*, **15**, 1832–1854.

Zeng, Q-C, X. D. Zeng, A. H. Wang, R. E. Dickinson, X. B. Zeng, and S. S. P. Shen, 2003a: Models and numerical simulations of atmosphere-vegetation-soil interaction and ecosystem dynamics. invited paper. Proceedings of ICCP6-CCP2003, Rinton Press Inc., Beijing.

Zeng, X. D., S. S. P. Shen, X. B. Zeng, and Q-C. Zeng, 2003b: A three-variable ecosystem model and its numerical simulations. Proceedings of ICCP6-CCP2003, Rinton Press Inc., Beijing.

Zeng, X. D., S. S. P. Shen, X. B. Zeng, and R. E. Dickinson, 2004: Multiple equilibrium states and the abrupt transitions in a dynamical system of soil water interacting with vegetation. *Geophys. Res. Lett.*, **31**, 5501, doi: 10.1029/2003 GL 018910.

Zeng Xiaodong, Wang Aihui, Zhao Gang, S. S. P. Shen, Xubin Zeng, and Zeng Qingcun, 2005a: Ecological dynamic model of grassland and its practical verification. *Science in China* (C), **48**, 41–48.

Zeng, X. D., X. B. Zeng, S. S. P. Shen, R. E. Dickinson, and Q-C. Zeng, 2005b: The vegetation-soil water interaction within a dynamical ecosystem model of grassland in semi-arid areas. *Tellus* (B), **57**, 189–202.